Compact physical model for simulation of thermal networks

Energy 175 (2019) 998–1008

Contents lists available at ScienceDirect

Energy

journal homepage: www.elsevier.com/locate/energy

Compact physical model for simulation of thermal networks

Elisa Guelpa*, Vittorio Verda

[a] Energy Department, Politecnico di Torino, Corso Duca Degli Abruzzi 24, 10129, Torino, Italy

ARTICLE INFO

Article history:
Received 31 December 2018
Received in revised form
4 March 2019
Accepted 10 March 2019
Available online 11 March 2019

Keywords:
Network management
Modelling
Smart energy systems
District heating
Multi energy system

ABSTRACT

Optimal design and management of DH networks require numerical models for simulating the physical behavior of the network in various operating conditions. DH network models usually rely on the physical description of the fluid-dynamic and thermal behaviours. The use of physical models can represent a limitation in various cases: a) when extended networks are considered (several thousands of nodes); b) when multiple simulations are required in real-time; c) when multi-energy networks are optimized. In these cases, compact models are preferable.

This work aims at presenting the compact model for fast simulation of thermal transients. The model preserves the reliability of a physical model because it solves the mass and energy equation. Only the momentum equation is simplified in order to overcome complexity related to the iterative solution of mass and momentum equations, which are coupled.

Results of the application to a real network show that the proposed methodology significantly reduces computational costs with respect to a complete physical model, with small impact on the accuracy. The approach is suitable for being used in combination with other network models (gas, electricity) and with models of other energy infrastructures, such as plants, storage units or energy conversion systems.

1. Introduction

District heating and cooling (DHC) is becoming a pillar of energy efficiency and decarbonization, because of the possibility of integrating renewable sources [1–3], waste heat [4–6] and highly efficient plants [7,8] for house heating/cooling and domestic hot water production. This technology is particularly convenient in the case of densely populated areas [9,10], where the advantages related with efficient heat production are larger than the distribution losses.

Network modelling is a crucial aspect related to the management of DHC systems. This is because:

- thermal transients are not negligible, especially in large networks, and should be taken into account for planning smart management of DHC systems;
- thermal losses may significantly affect the temperature distribution in the network, particularly in the case of low thermal loads;
- mass flow distributions vary considerably, depending on the thermal demand, the position of the operating plants and the pumping strategy.

DHC models are thus necessary in order to quantify which are the effects on the overall system efficiency of:

1. *Changes on the management of energy conversion units* [11,12] *and pumping systems* [13,14]. Changes in pumping strategy have been shown to affect primary energy saving about 1% of the primary energy required to a DHC system [13,14]. Production units should be properly selected based on their availability and instant production costs.
2. *Impact on storage installation/location.* Location of storage in strategic areas can increase the overall system efficiency and allow connecting further buildings at the network by overcoming limitations due to the pipeline diameters [15].
3. *Demand response application.* This concerns the change in the thermal request profiles of the buildings in order to modify the overall request. Application of virtual storage has been shown being successful for the reduction of the thermal peaks, by providing cuts from 5% to 25% and primary energy saving between 3.5% and 5%, in the cases of small and more advanced changes, respectively [16–19].

* Corresponding author.
E-mail address: elisa.guelpa@polito.it (E. Guelpa).

https://doi.org/10.1016/j.energy.2019.03.064

4. *Exploitation of the pipeline thermal inertia.* Smart management of the network operations enable the exploitation of the thermal inertia of the vector carrier inside the pipeline as a storage system [20–22].
5. *Modifications of the network topology.* These are mainly due to modifications of the pipeline design [23–25], or connection of additional buildings [26] to the DHC system.
6. *Effects of failure events.* It has been shown in Ref. [27] that a different management of the pumping system and plant operations provides significant reduction of the effect of pump failure and pipe leakages in DH networks.

The modelling approaches used for DHC networks can be grouped into physical and black box approaches.

The latter consists in creating a function (or combination of functions) by data interpolation. These are usually experimental data but also data obtained by physical model simulations. The strength of this type of model is the low computational time required to obtain solutions. Nevertheless, black box approaches are not suitable for predicting the network behavior in conditions not available in the dataset because lower accuracy might be obtained in the case an extrapolation is required. This reduces their range of applicability.

Physical models consist in the definition and the solution of physical problems on a computational domain, in a certain period. Physical models rely on the topological description of the network (connection between nodes and branches, locations of plants, user and pumping stations, etc.); these provide mass flows, pressures and temperature distributions within the network. Both of them require the prediction of the DHC system thermal demand [28].

Concerning DHC network models, various approaches have been proposed in the literature [29–31]. The main limitations related with the use of thermo-fluid dynamic models is due to the high computational time required to solve the physical problem. The issue of high computational costs arises for two main reasons:

- Circulation of the water within the network is evaluated through solution of mass and momentum conservation equations. These are particularly time consuming because of the non-linearities and therefore a guess and correction method must be used;
- The problem is usually applied to large computational domains. In case of DHC systems, the domain often refers to the entire network, which might be easily composed of various hundreds/thousands nodes. This is also the size of the equation set to be solved.

Reduction in the computational cost can be obtained by acting on one of the two above mentioned points.

Concerning the second point, two aggregation methods have been proposed: the German aggregation method [32] and the Denmark aggregation method [33]. These two methods have been compared in Ref. [34]. They aim at simplifying the network topology, by consequentially deleting nodes and branches of the network. In the end, an equivalent network results. The equivalent network has a thermo-fluid dynamic behavior as similar as desired to the real network. The main limitations of these approaches is related to their use for transient problems in looped network.

In Ref. [35], an approach that allows reducing the computational costs by splitting the computational domain into parts has been proposed. It works by solving the thermo-fluid dynamic problem separately for the various parts of the network by using an appropriate matching of boundary conditions. It allows to considerably reduce the computational cost and enable the possibility of using physical models also for very large systems (several thousands of branches).

In the present paper, a new methodology to keep the advantages of a physical model but reducing the computational cost is proposed. The approach acts on an alternative evaluation of the circulation of water within the pipelines. This is done by using the following approach:

- Water circulation within the network loops is computed through a black box approach, which takes into account the operating plants and the pumping station management;
- Thermal transients and mass flow distributions are obtained by solving conservation equations for mass and energy, i.e. by a physical approach.

The main strength of this work is to overcome the physical solution of the water circulation within the network by solving momentum conservation equations, which is very time consuming. Nevertheless the physical solution of mass and energy equations is preserved.

This leads to significant reductions of computational costs. However, some limitations exist. In fact, it is not possible to use this approach to study the installation of new plants or modifications in the network topology. In contrast, the approach can be successfully used for optimal management of storage units and thermal plants and for the analysis of demand response applications (virtual storage). In these cases, an optimal selection of the plant loads is crucial to increase the DHC system performances [36,37]. This is particular important when networks are fed with renewable sources, waste heat and heat pumps [38–40], and when are equipped with thermal storage systems [41–43].

In Section 2, a general physical problem for DHC network is described and the limitations related to the high computational cost are discussed. In Section 3, the innovative approach proposed in this paper is described. The test case is shown in Section 4. In Section 5, the results of the of fluid-dynamic and thermal analyses obtained comparing the compact approach and the full model are presented in terms of accuracy and computational cost.

2. General description of physical models for DHC networks

Physical description of DHC networks is usually made relying on one dimensional models, considering the main direction of water flow within the network pipelines. The network topology can be easily described by using a graph approach [44]: each pipe of the network is considered as branch starting from a node, the inlet node, and ending in another node, the outlet node. The connection between nodes and branches is obtained though the incidence matrix **A**. This matrix is composed by as many rows as the number of nodes and as many columns as the number of branches. A general element of the matrix, A_{ij}, is equal to 1 or -1 if the branch j enters or exits the node i and 0 otherwise.

The thermal fluid-dynamic model usually used for DHC networks includes the mass and energy conservation equations applied to all the nodes and the momentum conservation equation to all the branches. Water can be considered as an incompressible fluid and thermal conduction along each pipe is usually neglected. A general description of a physical model for DHC network is provided hereafter:

- The mass balance equation, in matrix form, allows evaluating the mass flow rates in each branch

$$G = g(A, G_{ext}) \quad (1)$$

where ***G*** is the vector including the mass flow rates in branches and

$\boldsymbol{G_{ext}}$ the vector of the mass flow rates exiting the nodes towards the extern. The latter has non-zero terms at the buildings and at the plants when an open network is considered, i.e. the supply network or the return network only.

- The steady-state momentum conservation equation can be used to evaluate pressures in the nodes:

$$\mathrm{P} = \mathrm{p}\left(\mathrm{A}, \mathrm{G}, \mathrm{N}, \Delta p_{pump}\right) \tag{2}$$

where $\boldsymbol{N}$ includes the characteristics of the pipeline (sections S, diameters D, lengths L, friction factor coefficients f, friction factors for concentrated losses β and global heat transfer coefficients U) and $\boldsymbol{\Delta p_{pump}}$ represents the pumping rise provided by the pumping stations located along the network.

Equations (1) and (2) are coupled because of the dependence of the pressure vector **P** on the mass flow rate vector **G**. In particular, the relation between P and G is nonlinear, as pressures depend on the square of mass flow rates, as can be seen in the extended equation provided in Table 1. Therefore, an iterative approach is required. Here a SIMPLE (semi implicit method for pressure linked equation) algorithm [45] is used, which is particularly suitable for solving Navier Strokes equations.

Momentum equation is usually written in steady state form because pressure perturbations travel the network at speed of sound, therefore the effects vanish in much smaller time than the time step used for the thermal transient solution.

- The energy conservation equation in a matrix form is:

$$\mathrm{T}(\tau) = \mathrm{t}\left(\mathrm{G}, \mathrm{T}(\tau - 1), \mathrm{N}, \mathrm{T}_{env}\right) \tag{3}$$

The energy equation is written in transient form because the thermal capacity cannot be neglected and the temperature perturbations travel the network at the speed of fluid.

Table 1 reports more in detail a physical model for the simulation of DHC networks [35]. The table also indicates the type of problems, the adopted approximations and the solution methods. Table 1 also shows the computational time required in order to solve an iteration of the problem for a network of 500 nodes (which corresponds to a medium size transport network). Cost appears quite low, but it is worth considering that they refer to a single iteration, while the mass, momentum and energy equations must be solved at each time steps. If the analysis of an entire day is required and a time step of 5 min is considered, the problem solution takes about 10 min. This time can be considered as acceptable for simulation purposes but there are applications in which this is not. Some examples are: a) optimizations, especially using heuristics approaches; b) multiple simulations for sensitivity analysis; c) analysis of possible actions to be performed in the case of malfunctions. Furthermore, in the case of large networks the computational cost dramatically increases, as indicated in Fig. 1.

3. Compact model description

3.1. Overall approach

Because of the large computational cost, it makes sense to develop methodologies which allow solving the problem within a reduced time.

Table 2 reports a summary of the equations to be solved in case of looped and tree-shaped network and when pressure distribution is required or not. When the aim is the evaluation of the thermal load or the temperature and mass flow distributions, knowledge of pressures is not strictly necessary. In the case of three-shaped networks, temperatures and mass flow rates can be obtained without solving the momentum equation. The latter can be solved in a post-processing mode, i.e. a sequential way which is much lighter than the solution of the entire equation set at once. In the case of looped networks, the solution of momentum equation is mandatory in order to evaluate the fluid circulation within the loops. This problem requires the implementation of an iterative approach because of the non linearities.

The main focus of this paper is an investigation on an alternative way to evaluate the water distribution in looped networks avoiding the solution of the momentum equation. An equivalent tree-shaped network is built by eliminating one branch per each loop. The water circulating the loops is computed by means of a black box model, which is trained with the results of simulations performed solving the full model or with measurements. These two steps are described in Sections 3.1.1 and 3.1.2.

3.1.1. Equivalent tree shaped network

The mathematical relation between nodes and branches in a network is expressed through the Euler's formula, reported in (4):

$$l = n - b + s \tag{4}$$

where l is the number of loops, n the number of nodes, b the

Table 1
DHC network model details.

	Mass conservation equation	Momentum conservation equation	ENERGY CONSERVATION EQUATION
Extended form	$\sum G_{in} - \sum G_{out} = G_{ext}$	$(\mathrm{p_{in}} - \mathrm{p_{out}}) = \frac{1}{2}\frac{\mathrm{f}}{\mathrm{D}}\mathrm{L}\frac{\mathrm{G}^2}{\rho \mathrm{S}^2} + \frac{1}{2}\sum_{\mathrm{k}}\beta_{\mathrm{k}}\frac{\mathrm{G}^2}{\rho \mathrm{S}^2} - \Delta \mathrm{p}_{pump}$	$\frac{\partial(\rho c \Delta T)_i}{\partial t}\Delta V_i + \sum_j c G_j T_j = U_{TOT}(T_i - T_{env})$
Function form	$\mathrm{G} = \mathrm{g}(\mathrm{A}, \mathrm{G_{ext}})$	$\mathrm{P} = \mathrm{p}(\mathrm{A}, \mathrm{G}, \mathrm{N}, \Delta \mathrm{p}_{pump})$	$\mathrm{T}(\tau) = \mathrm{t}(\mathrm{G}, \mathrm{T}(\tau - 1), \mathrm{N}, \mathrm{T}_{env})$
Matrix form	$\mathbf{A}\cdot\mathbf{G} + \mathbf{G_{ext}} = 0$	$\mathbf{G} = \mathbf{Y}\cdot\mathbf{A}^{\mathrm{T}}\cdot\mathbf{P} + \mathbf{Y}\cdot\boldsymbol{\Delta \mathbf{p}_{pump}}$	$\mathrm{M}\dot{\mathrm{T}} + \mathrm{KT} = \gamma$
Unknowns	**G** vector with mass flow rates in each branch	**P** vector with pressures in each node	**T** vector with temperatures in each node
Type of problem	• steady state • nonlinear coupled problem		• transient • linear problem
Approximations	• Water considered as incompressible • Velocity changes within a single pipeline neglected • The gravitational term in the static pressure		• Conduction along the pipelines is neglected
Solution Method	Simple algorithm		solver for linear equation system
Computational cost (for a 500 nodes network, 1 iteration)	About 2 s		About 1 s
Computational cost (for a 500 nodes network, 1 day)	About 10 min		About 4 min

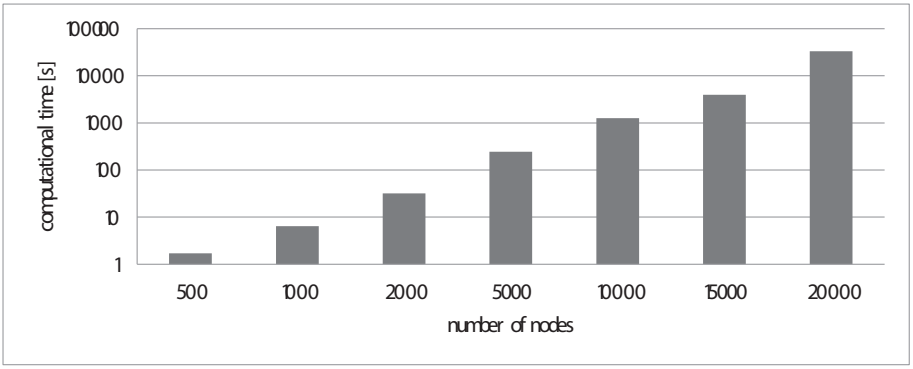

Fig. 1. Computational cost for solving mass and momentum conservation equation in DHC networks.

Table 2
Summary of the problem to be solved for different case of network types and requirements.

	Tree-shaped network	Looped network
Pressure distribution required	• mass conservation equation • momentum conservation equation • energy conservation equation	• mass conservation equation • momentum conservation equation • energy conservation equation
Pressure distribution not required	• mass conservation equation • momentum conservation equation (not required) • energy conservation equation	• mass conservation equation • momentum conservation equation (required for the evaluation of circulating flows in the loops) • energy conservation equation

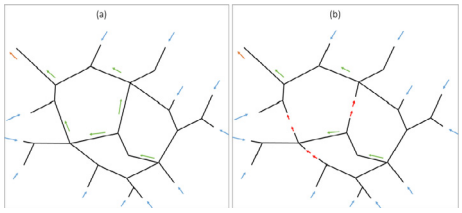

Fig. 2. a) looped network b) equivalent tree-shaped network.

number of branches and *s* the number of interconnected systems, which is 1 in case of a single DHC network.

From this relation it is clear that, starting from a looped network, it is possible to obtain a tree-shaped network by reducing the number of branches, without compromising the number of nodes and the number of interconnected systems. Therefore, the procedure requires that:

1. One branch for each loop is eliminated; the branch elimination does not affect the number of nodes nor the number of interconnected systems. This is indicated in Fig. 2b, which reports the creation of the equivalent three shaped network for an original network with 3 loops (2a);

2. The mass flow rate flowing the deleted branch is imposed as a boundary condition to the two end nodes of the branch. In particular an exiting flow is imposed in the inlet node of the examined branch and an entering flow is imposed in the outlet node of the examined branch (red arrows in Fig. 2b). The imposed mass flow rates are determined using the approach presented in the next section.

3.1.2. Evaluation of the mass flow circulating the loops (additional boundary conditions)

Once the equivalent network is build it is necessary to evaluate the mass flow circulating each loop. These are the additional boundary conditions of the systems. In the case no changes in the pumping strategy and in the network topology (including pipe closures due to malfunctions) are operated, the mass flow circulating each loop is only dependent on the mass flow rates processed at each thermal plant. The latter is a known piece of information during operation, since it is dependent on the thermal power supplied by each plant, which is part of the set of free variables in an optimal management problem. In this work, a regression model is used in order to relate the mass flow circulating the loops and the mass flow processed at each thermal plant. This is expressed as reported in eq. (5).

$$G_{ext\_add} = B \cdot G_{plant} \tag{5}$$

G_{ext_add} is the vector including the additional mass flows in the branches deleted, $\boldsymbol{B}$ is the regression coefficient matrix and G_{plant} is the vector including the mass flow rates processed at the various plants. The terms in **B** are obtained through linear interpolation of data obtained from measurements or full simulations. By the additional boundary conditions evaluated through (5) it is possible to easily solve energy and mass flow equations for tree shaped networks. This procedure significantly reduces the computational costs of the thermal fluid dynamic model but does not provide the pressure distribution along the network, since the solution of the momentum equation is overcome. Indeed the mass and energy conservation equation in the equivalent tree-shaped network are solved with the aim of calculating temperature and mass flow distributions in all the branches of the network using a physical approach.

3.2. Procedure implementation

A schematic of the overall procedure is presented in Fig. 3. The

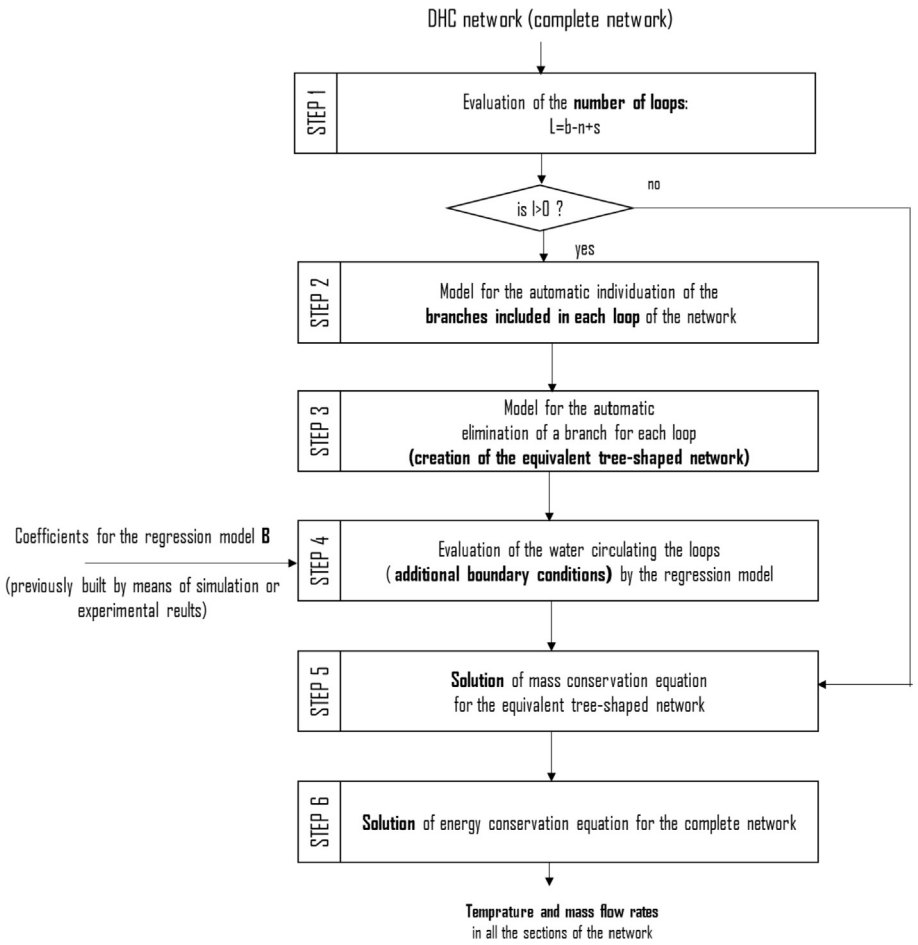

Fig. 3. Schematic of the model.

procedure includes the two steps previously discussed in Section 3.1.1 and section 3.1.2 and the various preprocessing stages.

At first, it is necessary to test if the DHC network analyzed includes some loops. If no loops are included, the momentum equation can be automatically overcome and the solution of energy and mass conservation equations can be directly obtained (from STEP 1 to STEP 5).

If the networks is looped, it is necessary to find the set of branches which constitute each loop. This is mandatory because the model should automatically open each loop in order to obtain the equivalent tree-shaped network. The list of branches constituting each loop is done by an iterative search. A routine is used to move along the network pipelines from a node to the consecutive one, starting from a thermal plant. The routine uses the incidence matrix. During the movement along the network, the list of branches in each path are stored in a vector. When a node is encountered twice, all the branches within the first and the second passage constitute a loop (STEP 2). Once the loop is found, one of the branches constituting the loop is randomly selected and is deleted, so that the loop is eliminated (STEP 3). This search is performed as many times as the number of loops included in the network.

Once the equivalent network is created, the additional boundary conditions are evaluated (STEP 4). This is done by means of the regression model, as discussed in Section 3.2.

The additional boundary conditions ($\mathbf{G_{ext\_add}}$) are included in the vector $\mathbf{G_{ext}}$, which becomes $\mathbf{G_{ext\_mod}}$ (as indicated in Table 1), while a different incidence matrix is created, excluding the deleted branched ($\mathbf{A_{mod}}$). By using $\mathbf{A_{mod}}$ and $\mathbf{G_{ext\_add}}$ it is possible solving the mass equation (STEP 5) to evaluate the mass flow rates in each branches of the tree-shaped network, by:

$$\mathbf{A}_{mod} \cdot \mathbf{G}_{tree\_shaped} + \mathbf{G}_{ext\_add} = 0 \tag{6}$$

The vector $\mathbf{G}$ including the mass flow rates of the initial looped network is obtained by including into $\mathbf{G_{tree\_shaped}}$, the additional mass flow included in $\mathbf{G_{ext\_add}}$.

Once mass flow rates in each node of the looped network are known, the energy equation is solved for the looped network; no differences in computational cost exist between tree-shaped and looped network, as the number of nodes is the same (STEP 6). This provides temperature distribution within the network pipelines.

4. Test case

The Turin network is selected as the test case for this new methodology. This is the largest network in Italy and one of the largest in Europe. The entire network pipeline is about 2500 km long; it includes more than 60000 nodes. The maximum thermal power request is over 1.3 GW, while the annual thermal request is 2000 GWh. Heat is produced in four thermal plants located in different areas of the network. There are 3 cogeneration groups, 4 groups of heat-only boilers and 3 groups of storage tanks, located in different areas of the network. The network supplies 5500

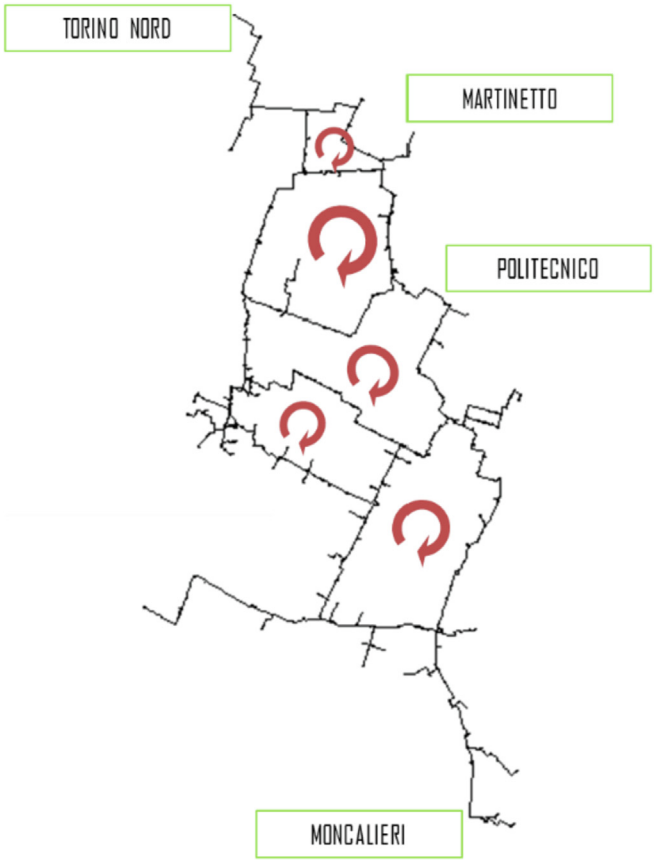

Fig. 4. Schematic o Turin transport line. In red the main loops.

buildings for a total volume of 56 million m^3. A schematic of the network is provided in Fig. 4. Water supply temperature is kept almost constant to about 120 °C during winter season.

DH networks can be considered as composed of two parts: the transport network, which is the portion of pipeline with large diameters linking the plants to the various areas, and the distribution networks, each linking the transport network to the buildings within the area. The nodes connecting the transport line to each distribution networks are also called barycentres. In the Turin network, there are 182 distribution networks. More details on the Turin network can be found in Ref. [35]. The methodology presented in this paper is applied to the transport network. This is 70 km long and it includes 9 loops, which allow limiting possible effects of failures as well as to allow better flow distribution and reducing pumping costs.

5. Results

5.1. Regression model

The regression model based on the mass flow rates processed by each thermal plant is an interesting alternative to the solution of the momentum equation because of the lower computational cost. Fig. 3 shows the mass flow circulating in the nine loops of the test case. Results obtained by means of the full model (consisting in the solution of the momentum and continuity equations) and the compact model (based on the regression model) are compared. Various scenarios in terms of thermal loads have been considered in the analysis (from 30%, to 100%) in order to examine the network in different conditions. Fig. 5 shows that mass flow rates evaluated with the two approaches are very similar in all the considered scenarios. This means that the compact model correctly detects the circulation of the flow within the pipelines.

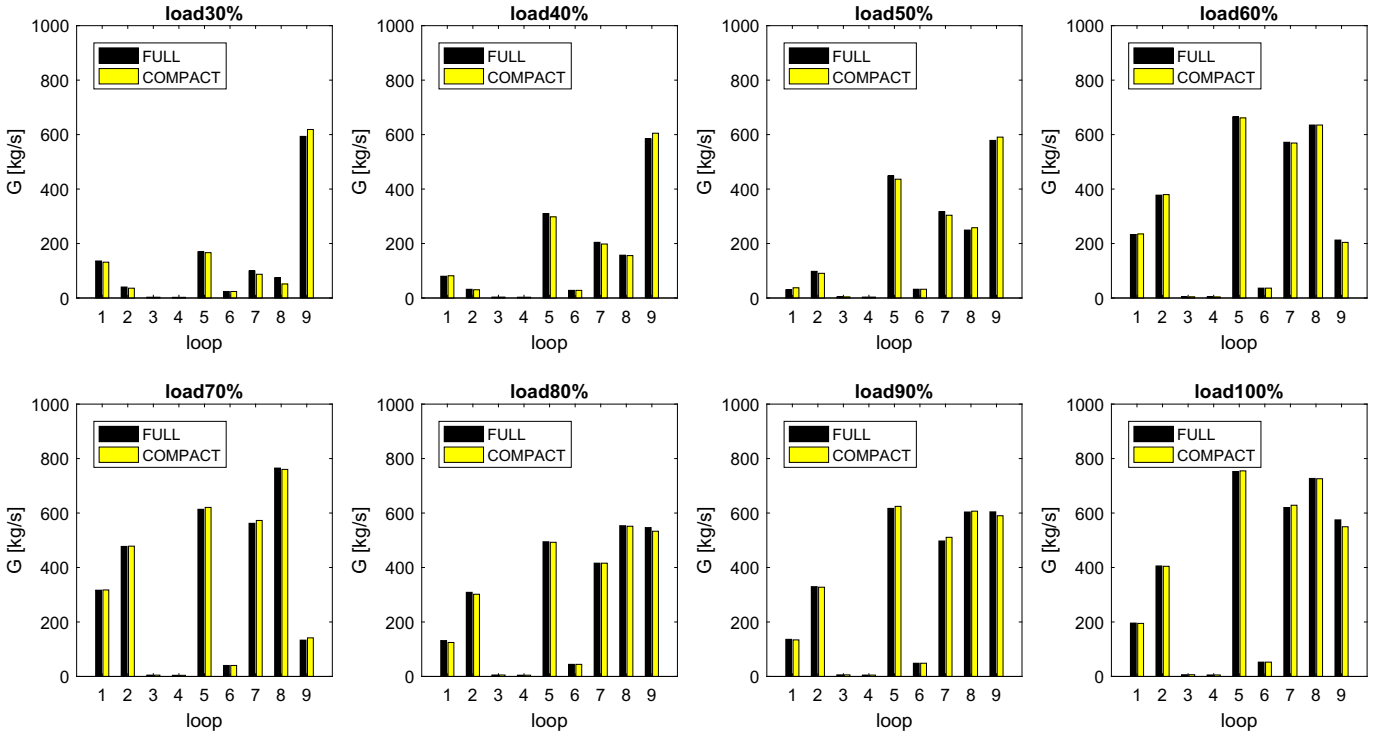

Fig. 5. Mass flow rates in the deleted branches, obtained through momentum and continuity equations (FULL) and regression model (COMPACT).

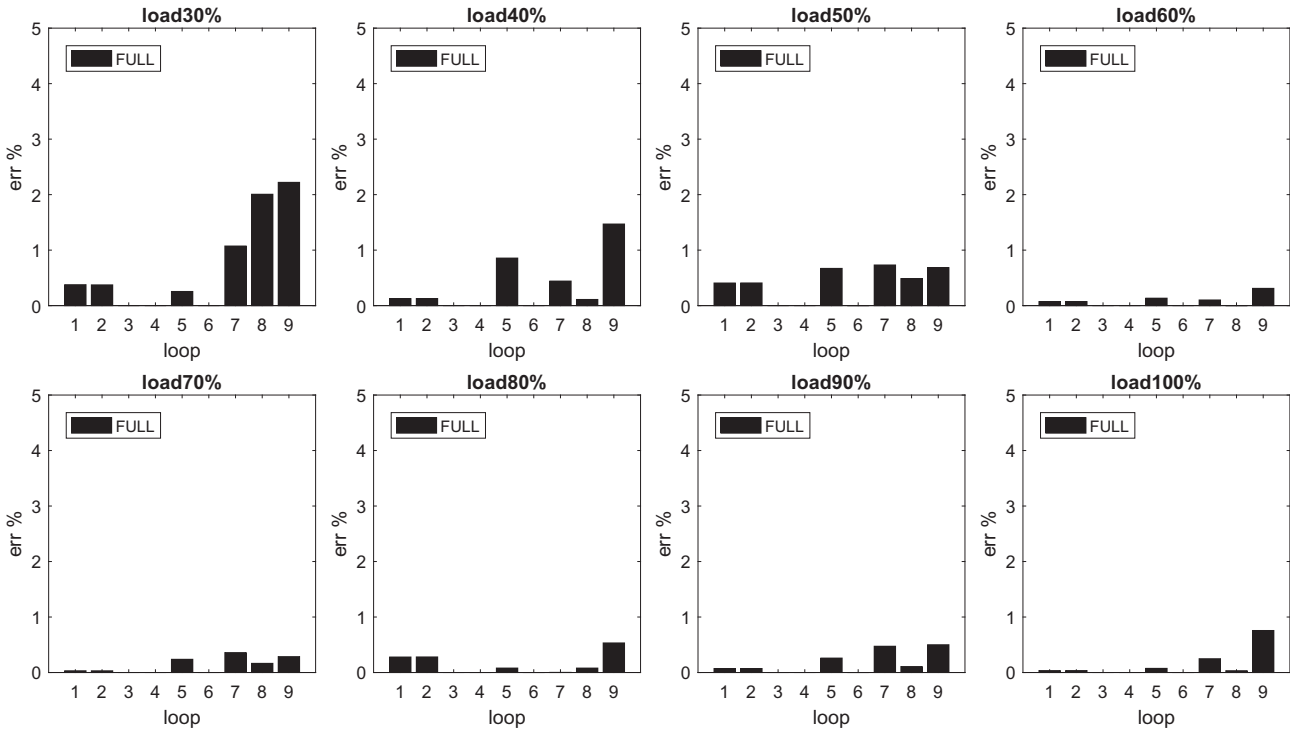

Fig. 6. Errors in mass flow rate evaluation.

The performances of the compact model are detailed in Fig. 6. The figure reports the relative error in the mass flow rate evaluation, calculated as:

$$err_i = \frac{G_{loop^i\_full} - G_{loop^i\_compact}}{\sum_{i=1}^{n_{loops}} G_{loop^i\_full}} \tag{6a}$$

This allows taking into account the magnitude of the relative error which is evaluated. In fact, in case of very low mass flow rates circulating a loop, the impact in the water circulation is very low although the relative error is high. Errors are lower than 5% for all the scenarios analyzed. This result is encouraging for the use of linear model to compute the circulation of mass flows in looped network.

5.2. Fluid dynamic results

In this section, results in terms of mass flow rates in the entire network are reported. Errors on the mass flows within the network indicate the effects of the errors made in the evaluation of the mass flow circulating the loops (Figs. 5 and 6) on water circulation. Fig. 7 shows the mass flow rate circulating within the transportation network in various scenarios. Results are reported for four of the eight scenarios previously considered (40%, 60%, 80% and 100%) for sake of simplification. Results obtained by both full and compact approaches are reported. Mass flows entering the network in the nodes corresponding with the thermal plants noticeably increase, while increasing the thermal load. This is can be noticed in case of mass flow entering the southern and northern branches (the

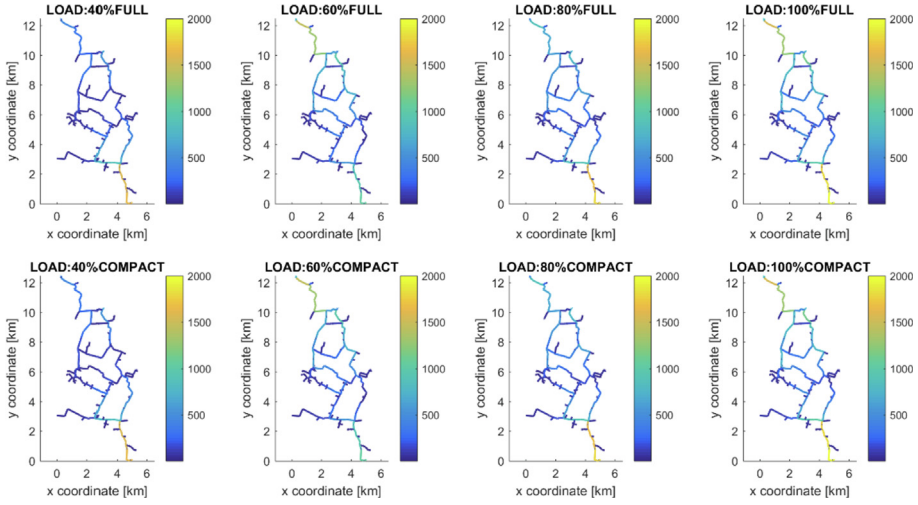

Fig. 7. Mass flow rate distribution [kg/s] in all the branches of the transport network.

Moncalieri and Torino Nord thermal plants, respectively). Mass flow rates predicted with the two approaches are very similar in all the branches of the network and for all the scenarios, with no significant differences, as shown in Fig. 4.

Fig. 8 reports the absolute error obtained in the mass flow evaluation through the compact model; this has been reported in all the branches of the network, for all the scenarios considered. The maximum deviation is 36 kg/s. This value is very low when compared with the mass flow rates circulating the network, which reaches about 2000 kg/s in the largest pipelines (Fig. 7). The average error, considering all the pipes in all the scenarios, is about 4 kg/s. This is about 0.1% of the maximum mass flow rate circulating in a branch of the network and 1% of the average mass flow rate circulating in the branches.

Fig. 9 shows the error made in the mass flow rate evaluation by using the compact model when compared to the full model in all the pipes of the network. Results are sorted in ascending order. Fig. 9 shows that the errors are mainly lower than 0.1 kg/s. The horizontal lines represent the absolute error of 10 kg/s and 50 kg/s, respectively. All the errors in all the scenarios are lower than 50 kg/s. On average, errors are lower than 10 kg/s in 70–90% of the branches for the various scenarios.

Concerning the computational cost, for the considered network the full model requires about 2 s for computing a time step on a single 3.3 GHz CPU. For the same network an iteration of the compact model requires about 0.0015 s. Ratio between the computational time is thus about 10^{-3}. Comparisons between computational costs required by the full and the compact model for networks with different dimensions (as a function of the number of nodes) are reported in Fig. 10. Computational cost saving is about 99% for all the network sizes (it reduces of two orders of magnitude).

5.3. Thermal results

Temperature distribution in the network nodes are reported in Fig. 11. The temperature in the upper part of the figure are evaluated relying on the mass flow rates are calculated with the full model. The temperature in the lower part of the figure are evaluated by means of the mass flow rates calculated with the compact model. As for the mass flow comparison, results are reported for four of the eight scenarios previously considered (40%, 60%, 80% and 100%) in order to easier visualize them.

Temperature values are higher near the power plants, while

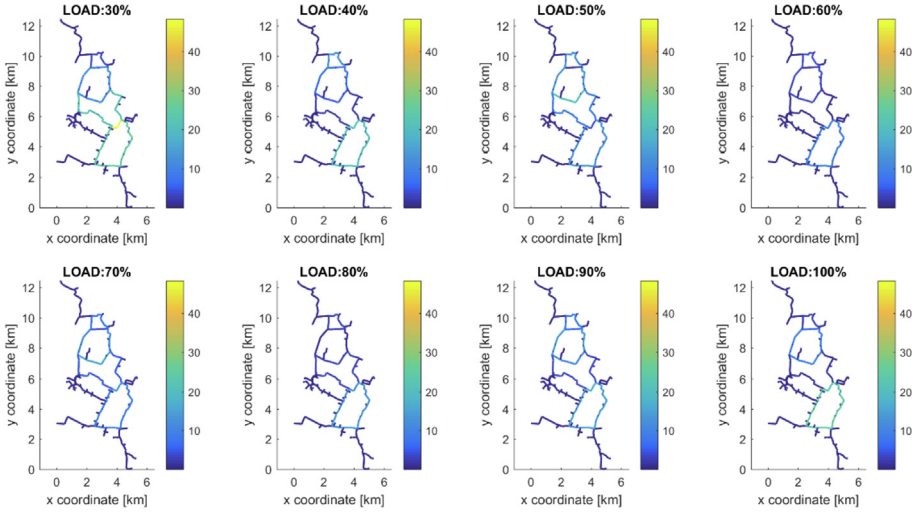

Fig. 8. Absolute error in the evaluation of mass flow [kg/s] in the transport network.

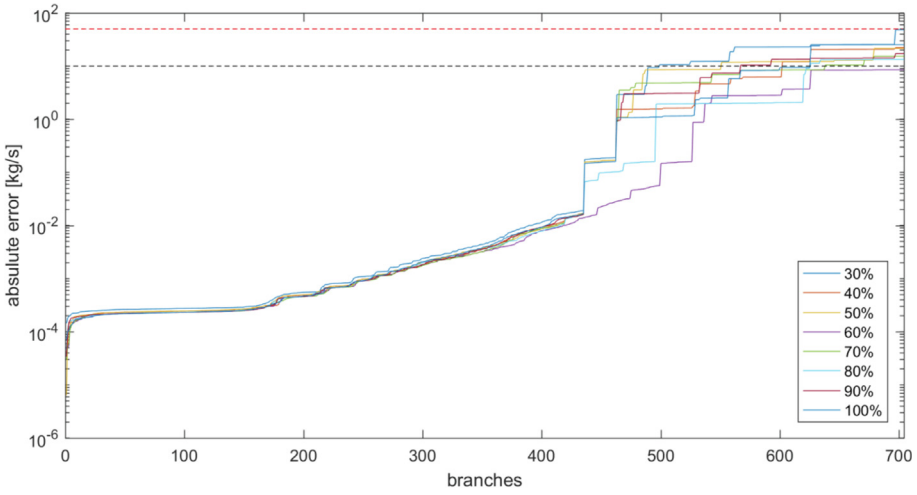

Fig. 9. Absolute error in the evaluation of mass flow [kg/s] in the transport network.

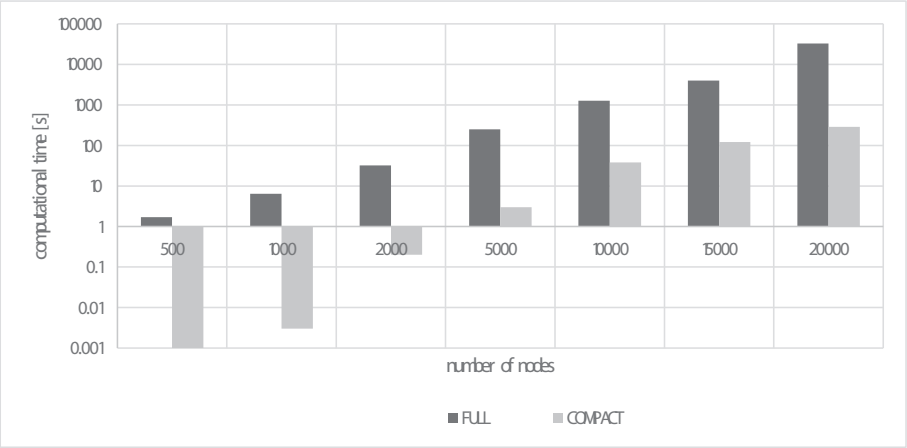

Fig. 10. Computational cost comparison.

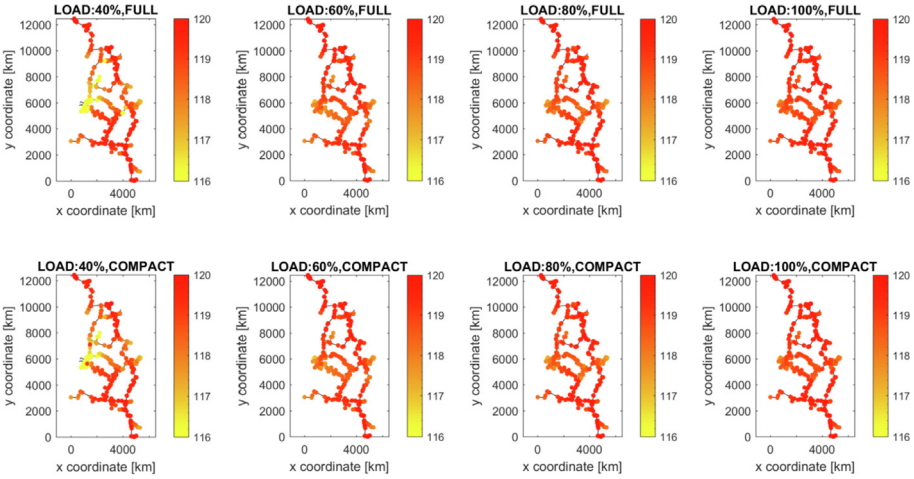

Fig. 11. Temperature [°C] in the transport network.

these reduce by moving away from the thermal plants. This is can be noticed in the nodes near Moncalieri and Torino Nord thermal plants, which are respectively on the north and south of the network. In case of very low mass flow rates, temperature tend to dramatically decrease. For this reason some nodes, where mass flows exceed the minimum limitation, are not plotted in the figure.

Results show that temperature values are quite similar in case of mass flow rates calculated with the full model and the compact model. Observing the various loops, it is possible to notice that no significant differences occur in each node of the network and in the various scenarios.

Fig. 12 shows the absolute errors computed in the scenarios plotted in Fig. 9. Maximum deviation occurs in scenario 30%; maximum value is around 3 °C. This value is obtained in the branches where the mass flows are very low and the thermal losses varies although the mass flow variation is small in module. The only areas where the errors are higher than 1 °C is the center/east area for the scenario 30%. This area is an industrial site that is no more connected to the DH and only few buildings in the area require heat. In this area, mass flow rates are low (see Fig. 7) and thermal losses (and consequently temperatures) vary significantly when mass flow rates slightly modify. The average absolute error is 0.07 °C. This value is negligible for the considered application and it clearly prove that the approximation deriving from the use of the compact model on the thermal distribution is quite low.

6. Conclusions

The present paper provides a compact physical approach for fast modelling of the fluid dynamic and thermal problems in DH networks. The model relies on the main strengths of both physical and black box approaches: the circulation of the mass flows in the loops is performed by using a regression model, avoiding the time consuming iterative solution of momentum equation, while mass flows and temperatures are evaluated by solving the continuity and energy equations. These allow obtaining mass flow rate and temperature evolutions in all the nodes of the network with reduced computational resources.

The model is based on two main ideas:

- an equivalent tree-shaped network is created instead of a looped network. This allows overcoming the necessity of solving the momentum equation.
- water flow rates in the eliminated branches are calculated through a black box approach. A linear model is adopted in this paper. Coefficients are obtained through solution of the full fluid dynamic problem or through measurements. Alternatively nonlinear polynomials or artificial neural networks can be used.

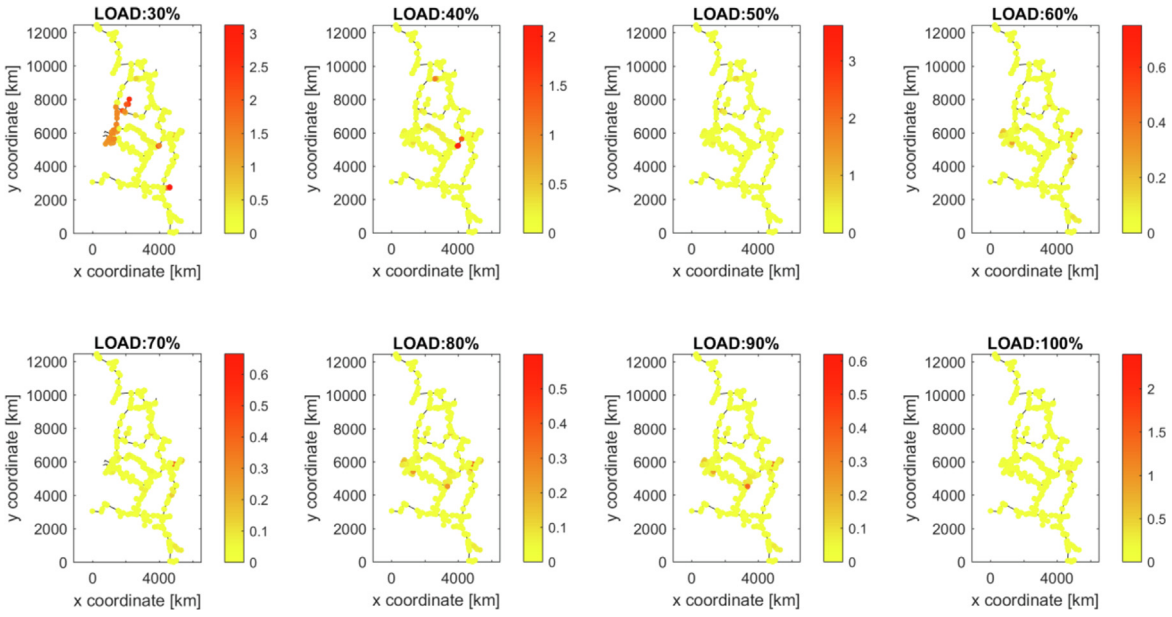

Fig. 12. Absolute errors in the temperature [°C] in the transport network.

This process avoids high computational costs required to the solution of the continuity and momentum equations, which coupling generates a non-linear equation set.

The approach has been tested to the Turin transport network. A detailed comparison between the full model (including the momentum equation) and the compact model is proposed. In particular the following results are presented: a) comparison of the mass flow rates circulating the loops, b) comparison of the mass flow rates in all the pipes of the network c) comparison of the temperatures in all the pipes of the network. The compact model well detects the water distribution in the loops of the network and the effects of the errors in the evaluation of the other mass flow rates within the network are negligible.

The computational cost to solve the fluid-dynamic model (full model) applied to the entire network is reduced by three orders of magnitude, which makes the approach suitable for optimizations and multi-scenario simulations, as well as for the analysis of very large networks.

Acknowledgments

This work has been conducted within the project PLANET “Planning and operational tools for optimising energy flows and synergies between energy networks”, funded by the European Union's Horizon 2020 Research and Innovation Programme under grant agreement no 773839 (topic: LCE-05-2017). The general aim of the PLANET project is to design and develop a holistic Decision Support System for grid operational planning and management in order to explore, identify, evaluate and quantitatively assess optimal strategies to deploy, integrate and operate conversion/storage systems on the distribution grid of several energy carriers.

Nomenclature

A	incidence matrix
B	matrix of linear interpolation coefficients
b	branches number
c	specific heat, J/(kg K)
D	pipe diameter, m
f	distributed friction factor
G	mass flow rate, kg/s
G	vector of mass flow rates
$\mathbf{G_{ext}}$	vector of mass flow rates extracted from nodes
k	thermal conductivity, W/(mK)
K	stiffness matrix
l	loop number
L	pipe length, m
M	mass matrix
n	node number
N	matrix of network characteristics
p	pressure, Pa
P	pressure matrix, Pa
P	vector of pressures
s	subsystem number
S	pipe section, m^2
t	time, s
T	temperature, °C
T	vector of temperatures
U	pipe transmittance, W/kg K
V	volume, m^3
Y	fluid dynamic conductance, kg/s/Pa
Y	matrix of fluid dynamic conductances

Greek symbols

β	localized friction factor
Δp_{pump}:	pressure rise in pumps, Pa
γ	known term in the energy equation
ρ	density, kg/m^3
τ	time, s
Φ	heat flux, W

Subscripts and superscripts

env	environmental
in	inlet
out	output

References

[1] Fahlén E, Ahlgren EO. Assessment of integration of different biomass

gasification alternatives in a district-heating system. Energy 2009;34(12):2184–95.
[2] Lindenberger D, Bruckner T, Groscurth HM, Kümmel R. Optimization of solar district heating systems: seasonal storage, heat pumps, and cogeneration. Energy 2000;25(7):591–608.
[3] Yildirim N, Toksoy M, Gokcen G. Piping network design of geothermal district heating systems: case study for a university campus. Energy 2010;35(8):3256–62.
[4] Fang H, Xia J, Zhu K, Su Y, Jiang Y. Industrial waste heat utilization for low temperature district heating. Energy Policy 2013;62:236–46.
[5] Holmgren K. Role of a district-heating network as a user of waste-heat supply from various sources–the case of Göteborg. Appl Energy 2006;83(12):1351–67.
[6] Fang H, Xia J, Zhu K, Su Y, Jiang Y. Industrial waste heat utilization for low temperature district heating. Energy Policy 2013;62:236–46.
[7] Casisi M, Pinamonti P, Reini M. Optimal lay-out and operation of combined heat & power (CHP) distributed generation systems. Energy 2009;34(12):2175–83.
[8] Ziębik A, Gładysz P. Optimal coefficient of the share of cogeneration in district heating systems. Energy 2012;45(1):220–7.
[9] Lund H, Moller B, Mathiesen BV, Dyrelund A. The role of district heating in future renewable energy systems. Energy 2010;35:1381–90.
[10] Werner S. International review of district heating and cooling. Energy 2017;137:617–31.
[11] Jing ZX, Jiang XS, Wu QH, Tang WH, Hua B. Modelling and optimal operation of a small-scale integrated energy based district heating and cooling system. Energy 2014;73:399–415.
[12] Gambino G, Verrilli F, Canelli M, Russo A, Himanka M, Sasso M, …, Glielmo L. Optimal operation of a district heating power plant with thermal energy storage. In: American control conference (ACC), 2016. IEEE; 2016, July. p. 2334–9.
[13] Sciacovelli A, Guelpa E, Verda V. November). Pumping cost minimization in an existing district heating network. In: ASME 2013 international mechanical engineering congress and exposition. American Society of Mechanical Engineers; 2013. V06AT07A066-V06AT07A066.
[14] Guelpa E, Toro C, Sciacovelli A, Melli R, Sciubba E, Verda V. Optimal operation of large district heating networks through fast fluid-dynamic simulation. Energy 2016;102:586–95.
[15] Söderman J. Optimisation of structure and operation of district cooling networks in urban regions. Appl Therm Eng 2007;27:2665–76.
[16] Guelpa E, Barbero G, Sciacovelli A, Verda V. Peak-shaving in district heating systems through optimal management of the thermal request of buildings. Energy 2017;137:706–14.
[17] Verda V, Guelpa E, Sciacovelli A, Patti E, Acquaviva A. Thermal peak load shaving through users request variations. Int J Thermodyn 2016;19(3):168–76.
[18] Guelpa E, Deputato S, Verda V. Thermal request optimization in district heating networks using a clustering approach. Appl Energy 2018;228:608–17.
[19] Verda V, Capone M, Guelpa E. Optimal operation of district heating networks through demand response. Int J Thermodyn 2019;22(1):35–43.
[20] Li Z, Wu W, Shahidehpour M, Wang J, Zhang B. Combined heat and power dispatch considering pipeline energy storage of district heating network. IEEE Trans Sustain Energy 2016;7(1):12–22.
[21] Basciotti D, Judex F, Pol O, Schmidt RR. November). Sensible heat storage in district heating networks: a novel control strategy using the network as storage. In: Conference proceedings of the 6th international renewable energy storage conference IRES; 2011.
[22] Yu J, Shen X, Sheng T, Sun H, Xiong W, Tang L. November). Wind-CHP generation aggregation with storage capability of district heating network. In: Energy internet and energy system integration (EI2), 2017 IEEE conference on. IEEE; 2017. p. 1–6.
[23] Dalla Rosa A, Li H, Svendsen S. Method for optimal design of pipes for low-energy district heating, with focus on heat losses. Energy 2011;36(5):2407–18.
[24] Vallios I, Tsoutsos T, Papadakis G. Design of biomass district heating systems. Biomass Bioenergy 2009;33(4):659–78.
[25] Yildirim N, Toksoy M, Gokcen G. Piping network design of geothermal district heating systems: case study for a university campus. Energy 2010;35(8):3256–62.
[26] Guelpa E, Mutani G, Todeschi V, Verda V. Reduction of CO2 emissions in urban areas through optimal expansion of existing district heating networks. J Clean Prod 2018;204:117–29.
[27] Guelpa E, Verda V. Model for optimal malfunction management in extended district heating networks. Appl Energy 2018;230:519–30.
[28] Guelpa E, Marincioni L, Verda V. Towards 4th generation district heating: prediction of building thermal load for optimal management. Energy 2019;171:510–22.
[29] Stevanovic VD, Prica S, Maslovaric B, Zivkovic B, Nikodijevic S. Efficient numerical method for district heating system hydraulics. Energy Convers Manag 2007;48(5):1536–43.
[30] Cross H. Analysis of flow in networks of conduits or conductors. University of Illinois at Urbana Champaign, College of Engineering. Engineering Experiment Station; 1936.
[31] Benonysson A, Bohm B, Ravn HF. Operational optimization in a district heating system. Energy Convers Manag 1995;36:297–314.
[32] Larsen HV, Pálsson H, Bøhm B, Ravn HF. Aggregated dynamic simulation model of district heating networks. Energy Convers Manag 2002;43(8):995–1019.
[33] Loewen A, Wigbels M, Althaus W, Augusiak A. A RenskiStructural simplification of complex DH-networks euroheat & power. 2001. p. 46–50.
[34] Larsen HV, Bøhm B, Wigbels M. A comparison of aggregated models for simulation and operational optimisation of district heating networks. Energy Convers Manag 2004;45(7–8):1119–39.
[35] Guelpa E, Sciacovelli A, Verda V. Thermo-fluid dynamic model of large district heating networks for the analysis of primary energy savings. Energy 2017. https://doi.org/10.1016/j.energy.2017.07.177. In press.
[36] Verrilli F, Parisio A, Glielmo L. Stochastic model predictive control for optimal energy management of district heating power plants. In: Decision and control (CDC), 2016 IEEE 55th conference on. IEEE; 2016, December. p. 807–12.
[37] Verrilli F, Srinivasan S, Gambino G, Canelli M, Himanka M, Del Vecchio C, …, Glielmo L. Model predictive control-based optimal operations of district heating system with thermal energy storage and flexible loads. IEEE Trans Autom Sci Eng 2017;14(2):547–57.
[38] Li Y, Fu L, Zhang S, Zhao X. A new type of district heating system based on distributed absorption heat pumps. Energy 2011;36(7):4570–6.
[39] Sciacovelli A, Guelpa E, Verda V. Multi-scale modeling of the environmental impact and energy performance of open-loop groundwater heat pumps in urban areas. Appl Therm Eng 2014;71(2):780–9.
[40] Aktaş M, Şevik S, Özdemir MB, Gönen E. Performance analysis and modeling of a closed-loop heat pump dryer for bay leaves using artificial neural network. Appl Therm Eng 2015;87:714–23.
[41] Bo H, Gustafsson EM, Setterwall F. Tetradecane and hexadecane binary mixtures as phase change materials (PCMs) for cool storage in district cooling systems. Energy 1999;24(12):1015–28.
[42] Sibbitt B, McClenahan D, Djebbar R, Thornton J, Wong B, Carriere J, Kokko J. The performance of a high solar fraction seasonal storage district heating system–five years of operation. Energy Procedia 2012;30:856–65.
[43] Sciacovelli A, Guelpa E, Verda V. Second law optimization of a PCM based latent heat thermal energy storage system with tree shaped fins. Int J Thermodyn 2014;17(3):145–54.
[44] Harary F. GraphTheory. New Delhi: Narosa Publishing House; 1995.
[45] PatankarS V. Numerical heat transfer and fluid flow. 1980.